

Analysis of double stub tuner control stability in a many element phased array antenna with strong cross-coupling

G.M. Wallace*, E. Fitzgerald*, J. Hillairet[†], D.K. Johnson*, A.D. Kanojia*, P. Koert*, Y. Lin*, R. Murray*, S. Shiraiwa*, D.R. Terry* and S.J. Wukitch*

*MIT Plasma Science and Fusion Center, Cambridge, MA 02139 USA

[†]CEA-IRFM, Saint-Paul-lez-Durance, France

Abstract. Active stub tuning with a fast ferrite tuner (FFT) allows for the system to respond dynamically to changes in the plasma impedance such as during the L-H transition or edge localized modes (ELMs), and has greatly increased the effectiveness of fusion ion cyclotron range of frequency systems. A high power waveguide double-stub tuner is under development for use with the Alcator C-Mod lower hybrid current drive (LHCD) system. Exact impedance matching with a double-stub is possible for a single radiating element under most load conditions, with the reflection coefficient reduced from Γ to Γ^2 in the “forbidden region.” The relative phase shift between adjacent columns of a LHCD antenna is critical for control of the launched $n_{||}$ spectrum. Adding a double-stub tuning network will perturb the phase of the forward wave particularly if the unmatched reflection coefficient is high. This effect can be compensated by adjusting the phase of the low power microwave drive for each klystron amplifier. Cross-coupling of the reflected power between columns of the launcher must also be considered. The problem is simulated by cascading a scattering matrix for the plasma provided by a linear coupling model with the measured launcher scattering matrix and that of the FFTs. The solution is advanced in an iterative manner similar to the time-dependent behavior of the real system. System performance is presented under a range of edge density conditions from under-dense to over-dense and a range of launched $n_{||}$.

*This work supported by US DoE cooperative agreement DE-FC02-99ER54512.

Keywords: LHCD, stub tuner, Alcator C-Mod, Lower Hybrid

PACS: 84.40.-x, 52.35.Hr, 52.50.Sw, 84.40.Dc, 84.40.Az

INTRODUCTION

Stub tuning networks have been used to reduce power reflected from the plasma on many fusion experiments in the ion cyclotron range of frequencies ($< \sim 100$ MHz) [1, 2] but have not yet been deployed at higher frequencies. A double stub matching network with electronically controlled tuning stubs is under development for the lower hybrid current drive (LHCD) system on Alcator C-Mod [3, 4]. The multijunction concept employed in many LHCD experiments reduces reflected power passively through destructive interference of the reflected waves, but at the cost of $n_{||}$ spectrum flexibility and control. An active matching network like a double stub tuner allows for complete control of the $n_{||}$ spectrum, in either the co- or counter-current direction, while reducing reflection coefficients to near zero.

The behavior of a single double-stub FFT connected in series with a mismatched load, Z_L , is well known. The matching network will reduce the input reflection coefficient, Γ_{in} , to zero for any load impedance outside the “forbidden region”, and from Γ_{in} to Γ_{in}^2 for load impedances inside the forbidden region. The problem is more complicated for a phased array LHCD antenna with strong cross-coupling between elements. The effective reflection coefficient for each element, Γ_n , is a function not only of the plasma density profile but also of the relative phase and amplitude of other nearby radiating elements. Mathematically, this can be expressed in terms of a series of matrix multiplication operations involving the scattering parameters of the plasma, antenna, and individual FFT elements.

SYSTEM DESCRIPTION

The plasma scattering matrix, S_p , is determined by the geometry of the antenna (primarily the waveguide height and septum thickness) and plasma (electron density, density gradient, and thickness of evanescent region). S_p is an $n \times n$ symmetric matrix, where n is the number of radiating elements in the antenna. The (n, n) elements are of order 0.2, while the $(n, n \pm 1)$ elements are of order 0.5. The magnitude of matrix elements decreases farther away from the diagonal since radiating elements spaced farther apart have weaker cross-coupling.

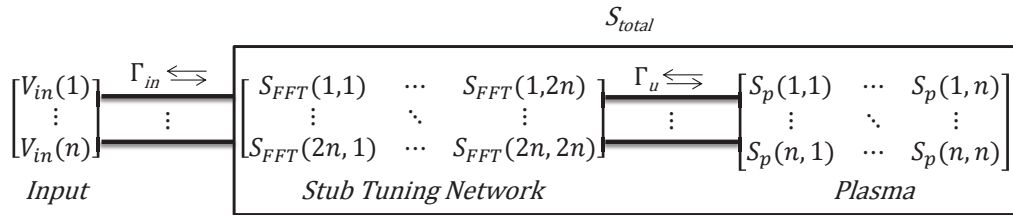


FIGURE 1. A block diagram of the network connections between the plasma scattering matrix, S_p , the FFT scattering matrix, S_{FFT} , and the input voltage vector, V_{in} .

The 2-port scattering matrix for a single FFT can be calculated given the reactive admittance of the two stubs, B_1 and B_2 , the wave propagation constant of the waveguide, β , and the distance between the stubs, l . The most straightforward way to determine this scattering matrix is to first cascade a series of three ABCD matrices representing the two stubs and the transmission line between the stubs. The S-matrix for the k^{th} FFT can then be calculated based on the four elements of the cascaded ABCD matrix. The individual S-matrices for the n FFTs are then combined into a larger $2n \times 2n$ S-matrix.

At this point, the two scattering matrices, S_p and S_{FFT} , can be cascaded [5] to get the total scattering matrix, S_{total} . Figure 1 shows a block diagram of the network connections between S_{FFT} and S_p to create S_{total} . Multiplying S_{total} by the driving waveform voltage vector V_{in} (e.g. $\{1, i, -1, -i, \dots\}$ for 90° phasing) gives the reflected wave for each input port of the combined FFT/plasma system. Since it is convenient to solve for the FFT stub lengths based on the reflection coefficient on the unmatched side of the FFT network, rather than the matched side, the unmatched reflection coefficient, Γ_u , must be calculated:

$$\Gamma_u = S_p V_{out} \oslash V_{out} \quad (1)$$

where \oslash represents the element-wise division of the column vector $S_p V_{out}$ by the column vector V_{out} and

$$V_{out} = [I_{n_{col}} - S_{FFT}(1:n_{col}, 1:n_{col})S_p]^{-1} S_{FFT}(1:n_{col}, n_{col}+1:2n_{col})V_{in} \quad (2)$$

Once Γ_u is calculated, the necessary reactive admittance of the two FFT stubs can be determined analytically [6]:

$$B_{1k} = -B_L + \frac{Y_0 \pm \sqrt{(1+t^2)G_L Y_0 - G_L^2 t^2}}{t}, B_{2k} = \frac{\pm Y_0 \sqrt{Y_0 G_L (1+t^2) - G_L^2 t^2} + G_L Y_0}{G_L t} \quad (3)$$

Here, $Y_k = G_L + iB_L$ is the normalized unmatched load admittance corresponding to the k^{th} element of Γ_u , and $t = \tan(\beta l)$. These new values for B_1 and B_2 are then inserted into S_{FFT} , and the process must be repeated. At each iteration Γ_u may change based on the new values of B_1 and B_2 for each column.

SIMULATION RESULTS

The system will be perfectly matched if the off-diagonal terms of S_p are zero and the load does not lie within the forbidden region. For an LHCD launcher the cross-coupling between waveguides is significant (higher, in fact, than the diagonal elements of S_p in most cases). In many cases the system converges quickly to a solution with very low reflection coefficients on the matched side, particularly when the off-diagonal terms of S_p are weak or $n_{col} \lesssim 4$. For larger, more coupled antenna arrays the system can be unstable if each FFT matching solution is calculated independently.

The behavior of the FFT/plasma system is studied here with a variety of plasma edge densities ($n_{co}, 2n_{co}, 5n_{co}$ where $n_{co} = 2.7 \times 10^{17} \text{ [m}^{-3}]$ is the cutoff density for 4.6 GHz LH waves), density gradients ($4.7 \times 10^{20}, 1.2 \times 10^{21}, 2.4 \times 10^{21} \text{ [m}^{-4}]$) and launched $n_{||}$ (1.63, 1.95, 2.60, 3.9; or $75^\circ, 90^\circ, 120^\circ, 180^\circ$ phasing). The plasma S-matrices used here are generated by the linear coupling code ALOHA [7]. Figure 2 shows the average matched reflection coefficient as a function of iteration number for a set of representative plasma conditions and phasings. The lowest and highest phasings exhibit unstable behavior under some conditions, while the reflection coefficient for moderate phasings drop quickly to very low levels.

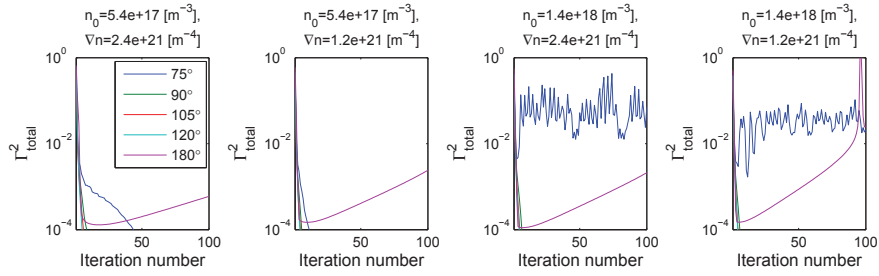


FIGURE 2. Overall power reflection coefficient Γ^2 of the LH FFT system for a single grill comprised of 16 columns. No spectrum compensation is used in this simulation. The gain, G , is 1 for this simulation.

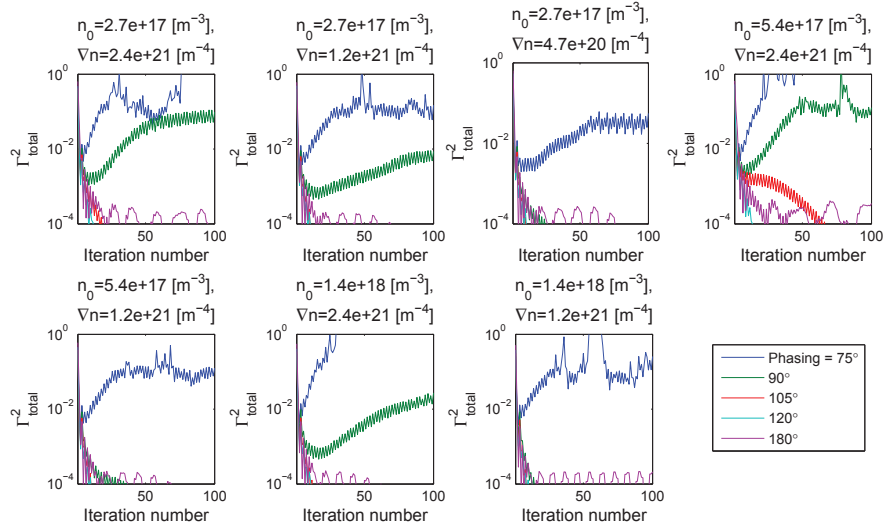


FIGURE 3. Overall power reflection coefficient Γ^2 of the LH FFT system for a single grill comprised of 16 columns. The phase and amplitude are compensated at every other iteration step. The gain, G , is 1 for this simulation.

The launched $n_{||}$ spectrum is also perturbed by the matching network. This effect can be compensated by adjusting V_{in} such that the magnitude and phase of V_{out} matches that of the desired drive waveform. This adjustment can also introduce instability in some circumstances. Figure 3 shows the same information as in Figure 2 but with the addition of phase and amplitude compensation for the forward wave of each column. This technique prevents distortion of the launched $n_{||}$ spectrum by adjusting V_{in} to achieve a constant amplitude and linear phase progression. The compensation process introduces additional instability for 75° and 90° phasings across a range of plasma loading scenarios.

Reducing the “gain” of the FFT control system can help to stabilize the response. Here, the gain, G , is defined as:

$$G = (B_{n+1} - B_n) / (B_{calc} - B_n) \quad (4)$$

where B_n is the stub reactive admittance at the n^{th} iteration, B_{n+1} is the programmed reactive admittance for the subsequent iteration, and B_{calc} is the calculated “ideal” reactive admittance for the subsequent iteration. The value of G represents the fractional amount of correction applied to the stub lengths between successive iterations. Figure 4 shows the effect of reducing the gain with spectrum compensation. Only 180° “heating” phasing shows instability with the gain reduced, while all other phasings exhibit stable behavior with average reflection coefficients less than 10^{-2} .

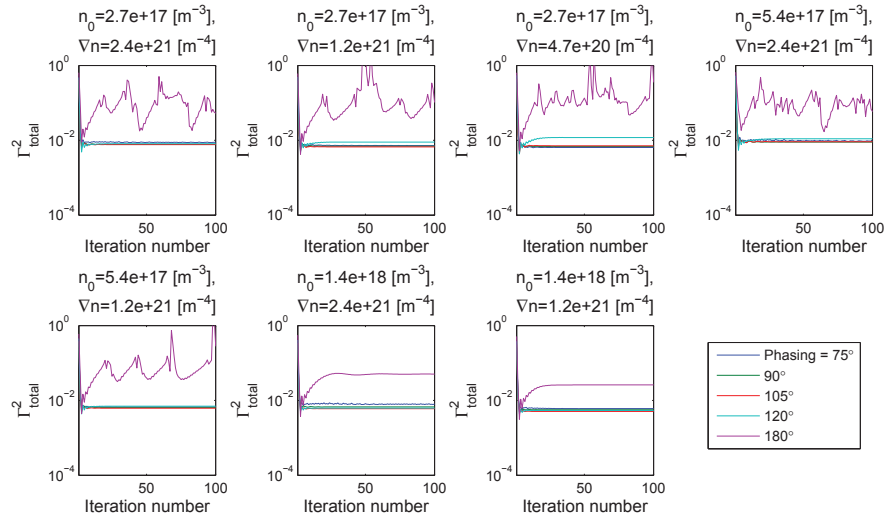


FIGURE 4. Overall power reflection coefficient Γ^2 of the LH FFT system for a single grill comprised of 16 columns. The phase and amplitude are compensated at every other iteration step. The gain, G , is 0.75 for this simulation.

DISCUSSION AND CONCLUSIONS

Decreasing the control system gain, G , is effectively equivalent to reducing the slew rate of the control coil current, or alternatively increasing the update rate of the reflection coefficient measurement/stub length calculation, with other parameters held constant. Effort has been expended to increase the slew rate of the electromagnet coil currents and decrease the penetration time for the resulting magnetic fields into the ferrite [8]. The simulations in this paper show that it may be necessary to slow down the response of the coils to avoid instability in the matching network.

Decreasing the gain has some negative impact on the final matched value of the reflection coefficient with an asymptote just under $\Gamma^2 = 10^{-2}$. With a gain of 1 and no spectrum compensation $\Gamma^2 < 10^{-4}$ in most cases. In practice a value of 10^{-2} is sufficiently low that the reflected power is negligible.

Uncertainty remains for the case of a time-varying plasma load. Future work will focus on this aspect of the FFT control system. The behavior of the FFT system with a time varying plasma load will set constraints on the necessary response time of the control system.

REFERENCES

1. R. Pinsker, *Plasma Physics and Controlled Fusion* **40**, A215 (1998), URL <http://iopscience.iop.org/0741-3335/40/8A/015>.
2. Y. Lin, A. Binus, and S. Wukitch, *Fusion Engineering and Design* **84**, 33 – 37 (2009), ISSN 0920-3796, URL <http://www.sciencedirect.com/science/article/pii/S0920379608002925>.
3. G. Wallace, S. Shiraiwa, J. Hillairet, M. Preynas, W. Beck, J. Casey, J. Doody, I. Faust, E. Fitzgerald, D. Johnson, A. Kanojia, P. Koert, C. Lau, Y. Lin, R. Leccacorvi, P. MacGibbon, O. Meneghini, R. Murray, R. Parker, D. Terry, R. Vieira, J. Wilson, S. Wukitch, and L. Zhou, *Nuclear Fusion* **53**, 073012 (2013), URL <http://stacks.iop.org/0029-5515/53/i=7/a=073012>.
4. P. Koert, D. Terry, E. Fitzgerald, P. MacGibbon, G. Wallace, and M. Takayasu, “Development of Fast Ferrite Tuner for Lower Hybrid current drive,” in *Fusion Engineering (SOFE), 2011 IEEE/NPSS 24th Symposium on*, 2011, pp. 1 –4, ISSN 1078-8891.
5. G. Simpson, “A Generalized n-Port Cascade Connection,” in *Microwave Symposium Digest, 1981 IEEE MTT-S International*, 1981, pp. 507–509, ISSN 0149-645X, URL <http://dx.doi.org/10.1109/MWSYM.1981.1129978>.
6. D. Pozar, *Microwave Engineering*, John Wiley & Sons, Inc., 1998.
7. J. Hillairet, D. Voyer, A. Ekedahl, M. Goniche, M. Kazda, O. Meneghini, D. Milanesio, and M. Preynas, *Nuclear Fusion* **50**, 125010 (2010), URL <http://iopscience.iop.org/0029-5515/50/12/125010>.
8. P. Koert, D. Terry, E. Fitzgerald, A. Kanojia, G. Wallace, R. Murray, and S. Wukitch, “Operation of a double stub tuner for Alcator C-Mod lower hybrid current drive system,” in *2013 Symposium on Fusion Engineering (SOFE)*, 2013.

AIP Conference Proceedings is copyrighted by AIP Publishing LLC (AIP). Reuse of AIP content is subject to the terms at: <http://scitation.aip.org/termsconditions>. For more information, see <http://publishing.aip.org/authors/rights-and-permissions>.